

## Optical characterization of Prodan aggregates in water medium†

Cite this: *Phys. Chem. Chem. Phys.*, 2013, **15**, 11800

Cíntia C. Vequi-Suplicy,\* Kaline Coutinho and M. Teresa Lamy

The fluorescent probe Prodan (2-dimethylamino-6-propionynaphthalene) has been widely used in biological systems, mainly due to the high sensitivity of its emission spectrum to the medium polarity. Though mostly used as a membrane probe, in lipid dispersions Prodan partitions in water, mainly in the presence of gel-phase bilayers. Here, optical properties of Prodan in aqueous medium are experimentally studied using absorption and emission spectroscopies, and compared with those of the probe in cyclohexane, where it is supposed to be very soluble. In parallel, theoretical calculations of the absorption spectrum of a monomer and aggregated Prodan in water were performed. Moreover, to understand Prodan–water and Prodan–Prodan interactions, solvation free energies of Prodan in water and in liquid Prodan were calculated. A light scattering profile underneath the optical absorption spectrum of Prodan in water clearly indicates the presence of aggregates at very low Prodan concentrations (0.9  $\mu\text{M}$ ). Experimental evidence of Prodan aggregation is theoretically supported by solvation free energy calculations, which demonstrate that Prodan molecules interact preferentially with other Prodan molecules than with water molecules. Theoretical calculations for electronic transition energies of monomers and aggregated Prodan in water show that a Prodan optical absorption band at 358 nm is related to the monomeric form of Prodan. This band saturates as Prodan concentration increases, indicating that aggregated Prodan prevails at higher concentrations. The relative increase in Prodan aggregated population is monitored by the increase in an absorption band at higher energies, at around 250 nm, and by the disappearance of a band at around 280 nm. Surprisingly, it was observed that the fluorescent emission spectrum of Prodan is not sensitive to probe aggregation up to around 15  $\mu\text{M}$ . Hence, Prodan aggregation in water medium, even at very low concentrations, must be considered when using this fluorescent probe in biological systems, having in mind that its fluorescence spectrum is rather insensitive to aggregation.

Received 26th April 2013,

Accepted 15th May 2013

DOI: 10.1039/c3cp51776d

[www.rsc.org/pccp](http://www.rsc.org/pccp)

### 1. Introduction

In the last few decades, biological molecules surrounded by different liquid solvents have been the object of many studies,<sup>1–7</sup> since in most biological systems molecules are embedded in fluids, especially water. From both experimental and theoretical points of view, a good description of the interaction between a given molecule and its environment is of fundamental importance to the understanding of its biological, chemical and physical properties.

Since it was designed by Weber and coworker,<sup>8</sup> Prodan (2-dimethylamino-6-propionynaphthalene) has been used as

a fluorescent probe to study several biologically relevant systems, such as membranes,<sup>9–24</sup> proteins,<sup>8,25–28</sup> and others.<sup>29–32</sup> Although widely used and studied, mostly as a lipid membrane probe, Prodan properties in different environments, both in the fundamental and excited states, are still controversial.<sup>10,11,33–59</sup> Prodan was designed to have a large charge separation between the nitrogen and the oxygen atoms placed at opposite positions in the naphthalene ring, to make the probe highly sensitive to the medium polarity (Fig. 1). This charge separation was also thought to increase the probe interaction with water molecules. But a recent theoretical study,<sup>60</sup> which presents the atomic charges of Prodan in three different environments (vacuum, cyclohexane and water), showed that the charge separation in water is not between the amine and carboxyl groups, but it occurs locally in the carboxyl group, between the oxygen and the carbon atoms. Also the presence of the highly hydrophobic naphthalene ring can decrease the interaction of Prodan with

*Instituto de Física, Universidade de São Paulo, SP, Brazil. E-mail: cintia@if.usp.br; Fax: +55 11 38134334; Tel: +55 11 30916661*

† Electronic supplementary information (ESI) available. See DOI: 10.1039/c3cp51776d

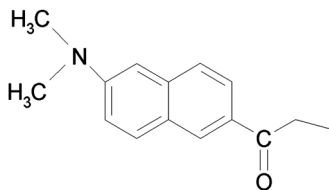


Fig. 1 Prodan molecular structure.

water molecules. So the hydrophobic–hydrophilic characteristics of Prodan are still an open question.

Considering this question, the present paper focuses on solubility properties of Prodan in water and in the non-polar solvent cyclohexane, through the study of the optical properties of the probe in the two solvents. It was reported that Prodan is aggregated in aqueous solution but only at concentrations higher than 10  $\mu\text{M}$ ,<sup>42,55</sup> and a fluorescent emission band at 430 nm was attributed to Prodan aggregates.<sup>55</sup> However the results presented here show that both statements are not correct.

Here, Prodan optical absorption and emission spectra were studied at different Prodan concentrations, in two solvents, water and cyclohexane. Parallel to that, theoretical calculations of the absorption spectra of a single Prodan molecule and Prodan aggregates, in water, were performed, and compared with the absorption spectrum at low and high molecular concentrations, respectively. Moreover, to understand Prodan–water and Prodan–Prodan interactions, solvation free energies of Prodan in water and in liquid Prodan were calculated. Considering the optical absorption spectrum of Prodan, we show that Prodan in water is aggregated at very low concentrations, namely 0.9  $\mu\text{M}$ , whereas the fluorescent probe in cyclohexane is monomeric up to 20  $\mu\text{M}$ . Theoretical calculations were found to be in accord with optical experimental results. Surprisingly, the fluorescent spectrum of Prodan was found to be rather unresponsive to Prodan aggregation, and no special emission band could be detected for aggregated Prodan in pure water, up to 20  $\mu\text{M}$ . To our knowledge, this is the first time that the Prodan optical spectrum is carefully studied as a function of Prodan concentration, in pure water medium.

## 2. Materials and methods

### 2.1 Experimental procedures

**2.1.1 Materials.** The fluorescent probe Prodan (Fig. 1) was purchased from Molecular Probes Inc. (Eugene, OR, USA) and the solvent cyclohexane from Sigma-Aldrich (St Louis, MO, USA). Water was from Milli-Q Plus (Millipore), pH  $\sim$  6.

**2.1.2 Sample preparation.** A stock solution of Prodan in chloroform or acetonitrile (1.5 mM) was used in all experiments. An appropriated amount of this solution was transferred to a glass flask, using a calibrated glass microsyringe. Chloroform (or acetonitrile) was evaporated under a stream of dry  $\text{N}_2$ . The dry residue was dissolved in the desired solvent (water or cyclohexane) to obtain the initial Prodan concentration of 20  $\mu\text{M}$ . Lower concentrations were obtained by the addition of pre-determinate volumes of the solvent. Before each measurement (for each concentration), the sample was stirred

and incubated for 10 minutes at room temperature, to assure that equilibrium had been achieved. pH was measured for all samples in water, and no alteration was observed when Prodan concentration was varied.

### 2.1.3 Electronic absorption and emission measurements.

Electronic absorption spectra were measured using a HP UV-Vis 8452A diode array spectrophotometer (Hewlett-Packard Co., Palo Alto, CA, USA), and temperature was kept at  $25 \pm 1$   $^\circ\text{C}$  using a Julabo F25-HP water bath (JULABO USA Inc., Allentown, PA, USA). The fluorescent emission spectrum and the steady state anisotropy were measured using a Varian Cary Eclipse Fluorescence spectrophotometer (Varian Australia PTY LTD, Mulgrave, VIC, Australia), with automated polarizers and a Peltier temperature controller (at 25  $^\circ\text{C}$ ). Prodan was excited at 360 and 340 nm, in water and cyclohexane, respectively. For fluorescence anisotropy measurements, the emission wavelength was set at 521 and 390 nm, for water and for cyclohexane, respectively. For all measurements, a quartz cuvette with an optical path of 1 cm was used.

The sample emission spectrum was measured right after the absorption spectrum, with no more than a few minutes between the two measurements. All data shown are means of the results of at least three experiments, and uncertainties are calculated standard deviations. If not shown, the uncertainty was found to be smaller than the symbol.

### 2.2 Theoretical calculations

**2.2.1 Electronic absorption energy calculations.** To calculate the electronic absorption transitions of Prodan in solution, the sequential hybrid method using Quantum Mechanics (QM) and Molecular Mechanics (S-QM/MM) was used.<sup>61,62</sup> Initially, a Monte Carlo (MC) simulation of the solution was performed and then relevant configurations of the solute–solvent system were selected to perform the QM calculation of the electronic absorption spectrum. All QM calculations were performed using the Gaussian03 program,<sup>63</sup> except for the absorption transition energies that used the semi-empirical method, Intermediate Neglect of Differential Overlap (INDO), with the spectroscopic parameterization method,<sup>64</sup> and single excitations calculated with Configuration Interaction (CIS), implemented in ZINDO program.<sup>65</sup> All the MC simulations were performed using the DICE program.<sup>66</sup>

The MC simulations were performed using the Metropolis sampling technique,<sup>67,68</sup> periodic boundary conditions, and the minimum image method, in the isothermal–isobaric  $NpT$  ensemble, where the number of molecules  $N$ , the pressure  $p$  and the temperature  $T$  are fixed.<sup>69</sup> Room temperature ( $T = 298$  K) and normal pressure ( $p = 1$  atm) were used for all simulations. Interacting potential was described by the Lennard-Jones (LJ) and Coulomb potentials, with three parameters for each atom  $i$  ( $\epsilon_i$ ,  $\sigma_i$  and  $q_i$ ).<sup>62</sup> For Prodan, the geometry was obtained with QM optimization using the Density Functional Theory (DFT) with the hybrid potential B3LYP,<sup>70,71</sup> and basis functions 6-31G(d) and 6-311+G(d,p).<sup>72</sup> Both sets of basis functions present the same planar structure as the Prodan molecule in the ground state, and this geometry is in good agreement with the X-ray structure.<sup>40</sup>

The LJ parameters,  $\epsilon_i$  and  $\sigma_i$  for the Prodan molecule, were obtained from the Optimized Potentials for the Liquid Simulations/All Atoms (OPLS/AA) force field,<sup>73</sup> the atomic charges were calculated using the QM second order perturbation method (MP2),<sup>74,75</sup> and the basis functions aug-cc-pVDZ,<sup>76</sup> in a vacuum and in water solution, as described in previous publication.<sup>60</sup> For water molecules, the used force field was the single point charge (SPC) model.<sup>77</sup>

Two systems were simulated: Prodan in aqueous solution and liquid Prodan. For Prodan in water, the system was composed of one Prodan molecule surrounded by 1000 water molecules. Since Prodan has one dimension bigger than the others, a rectangular box was chosen to keep approximately the same amount of water molecules at all directions around Prodan. The simulation consisted of a thermalization process of  $1.2 \times 10^8$  MC steps, followed by an equilibrium process of  $1.5 \times 10^8$  MC steps. In equilibrium, the average box dimensions were  $30.6 \times 36.6 \times 26.6$  Å, which gives an average density of  $1.029(8)$  g cm<sup>-3</sup>. For liquid Prodan, the system was composed of 250 Prodan molecules in a cubic box. The simulation consisted of a thermalization process of  $4.0 \times 10^8$  MC steps, followed by an equilibrium process of  $1.5 \times 10^8$  MC steps. In equilibrium, the average box size was  $46.2$  Å, which gives an average density of  $0.953(3)$  g cm<sup>-3</sup>.

After simulations, statistical analysis was performed,<sup>62</sup> and 75 configurations of the system with less than 10% of statistical correlation were selected and subjected to QM calculations. For the monomeric Prodan molecule in water, the electronic absorption transition energies were calculated in 75 statistically uncorrelated configurations composed of 1 explicit Prodan molecule embedded in the electrostatic field of 290 water molecules represented as point charges. To take into account the effect of the Prodan aggregation, the electronic absorption transition energies were calculated in 75 statistically uncorrelated configurations, composed of 2 explicit Prodan molecules (dimers selected from the liquid Prodan simulation) embedded in the electrostatic field of the self-consistent reaction field (SCRf) of the aqueous solution. The final values for electronic absorption transition energies were calculated as an average over 75 QM calculations. Absorption electronic energies for larger aggregates, with 3 to 10 Prodan molecules, were also calculated and the results were found to be similar to those of the dimer, only with the increase of the number of transitions at each electronic energy. Therefore, comparing the calculated absorption spectrum of the Prodan dimer and larger aggregates, no band shift was observed, but only an increase in band intensities. For computational reasons, the 75 calculations were performed for the dimer only, to obtain the mean values.

**2.2.2 Solvation free energy calculations.** To try to understand the interaction between Prodan–water and Prodan–Prodan, the solvation free energies of Prodan in water and in liquid Prodan were calculated using the thermodynamic perturbation theory (TPT),<sup>78–82</sup> implemented in the MC simulations.<sup>83,84</sup> The solvation free energy was calculated through a hypothetical process where solute–solvent interactions are switched-off in several simulations, using the double-wide sampling technique.<sup>81,85</sup>

Ten simulations were performed to make the solute molecule disappear in the solution: four simulations with double-wide sampling were performed to annihilate the Coulomb potential ( $\lambda q_i$  with  $\lambda = 1.00, 0.95, 0.90, 0.80, 0.70, 0.60, 0.40, 0.20$  and  $0.0$ ), three simulations with double-wide sampling to annihilate van der Waals interaction (attractive term of the LJ potential,  $r^{-6}$  with  $\lambda = 1.00, 0.75, 0.50, 0.40, 0.30, 0.20$  and  $0.00$ ), and three simulations without double-wide sampling to annihilate the cavitation term (repulsive term of the LJ potential,  $r^{-12}$  with  $\lambda = 1.00, 0.50, 0.25$  and  $0.00$ ). For each simulation  $1.20 \times 10^8$  MC steps were performed in the thermalization stage, and  $3.00 \times 10^8$  steps in the equilibrium. More details about this procedure can be found in ref. 83 and 84.

## 3. Results and discussion

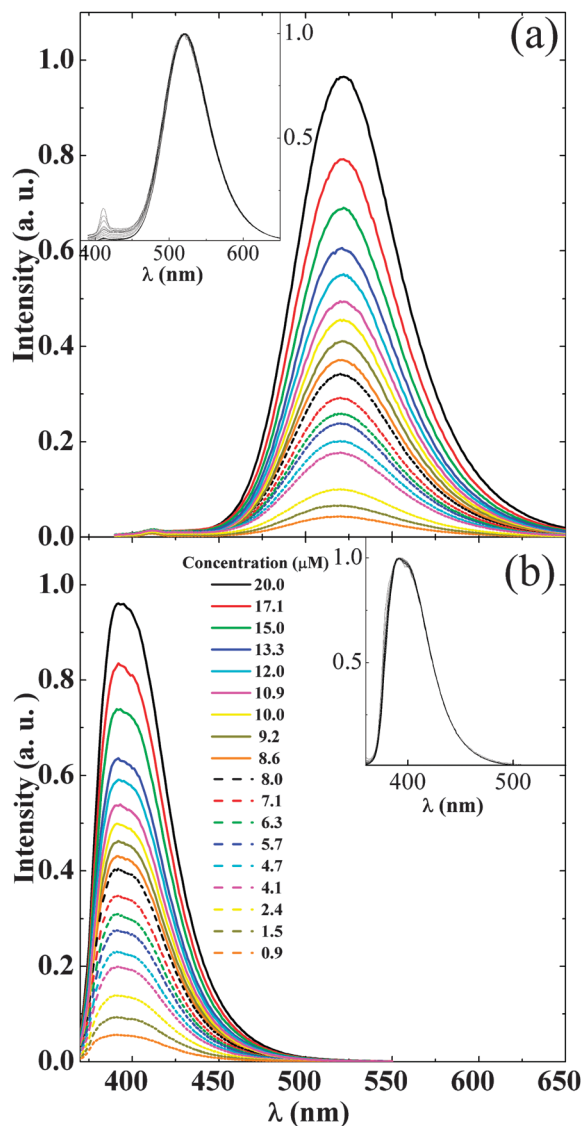
### 3.1 Prodan fluorescence

Fig. 2 shows the fluorescence emission spectra of Prodan in water (a) and in cyclohexane (b), as a function of the Prodan concentration. The spectrum maximum is at 522 nm for Prodan in water and 394 nm for Prodan in cyclohexane, in agreement with previous results.<sup>46,55,86</sup> In the studied concentration range, 0.9 to 20 μM, the shape of the fluorescent emission spectrum of Prodan is not concentration dependent, either in water ( $\epsilon = 78.9$ ) or in cyclohexane ( $\epsilon = 2.0$ ), as indicated by the superposition of all normalized fluorescence spectra (insets in Fig. 2).

It is important to stress that the previously reported emission band at 430 nm, detected in Prodan water solutions,<sup>42,55</sup> and attributed to aggregated Prodan,<sup>55</sup> was not detected in Prodan water solutions studied here (Fig. 2). As our samples were prepared in the total absence of organic solvent (see Materials and methods), this is in accord with the discussion made by Sun *et al.*,<sup>42</sup> who pointed out that the band at 430 nm was absent in water Prodan samples obtained after total evaporation of the organic solvent. Hence, it shall be due to Prodan–solvent interaction, and not to aggregated Prodan.

To better analyze the concentration dependence of the Prodan emission spectrum, in both solvents, Fig. 3 shows the area under the spectrum (proportional to the number of emitted photons) as a function of Prodan concentration. In water, up to around 15 μM, Prodan emission increases linearly with the concentration. In cyclohexane, the linear dependence between the concentration and the emission intensity goes up to the maximum concentration tested, 20 μM. That could be interpreted as an indication that the fluorophore is monomeric up to ~15 μM in water, and at least up to 20 μM in cyclohexane, as proposed before.<sup>42,55</sup> However, as discussed below, the Prodan optical absorption spectrum gives different information.

Prodan steady state fluorescence anisotropy was also monitored at all concentrations studied. Anisotropy values measured in both water and cyclohexane were found to be nearly independent of Prodan concentration (Fig. 4). This indicates that the dimensions of Prodan in solution, either monomeric or aggregated, do not change much with the probe concentration. If present, larger Prodan aggregates would tumble slower in solution, hence would yield higher fluorescence anisotropy values.<sup>86</sup> The higher



**Fig. 2** Emission spectra of Prodan in water (a) and in cyclohexane (b), at different concentrations. Insets show the superposition of all normalized spectra. Water:  $\lambda_{\text{exc}} = 360$  nm. Cyclohexane:  $\lambda_{\text{exc}} = 340$  nm. Temperature 25 °C.

anisotropy value observed for Prodan in cyclohexane (Fig. 4) could be due to lower Prodan excited state lifetimes found in this solvent: 0.6(1) and 2.1(2) ns in water as compared with 0.2(1) and 0.8(1) ns in cyclohexane, which are in good agreement with values reported before (Rowe *et al.*<sup>57</sup>).

### 3.2 Prodan electronic absorption

The electronic absorption spectra of Prodan in water and in cyclohexane are presented in Fig. 5. They were obtained over the same Prodan concentration range as the emission spectra shown in Fig. 3. In cyclohexane, as observed for the emission spectra (Fig. 3b, inset), the shape of the Prodan electronic absorption spectrum seems to be independent of its concentration (see normalized spectra in Fig. 5b, inset), and there is no obvious light scattering, up to 20  $\mu\text{M}$ , clearly indicating the presence of very small absorption centers, possibly Prodan

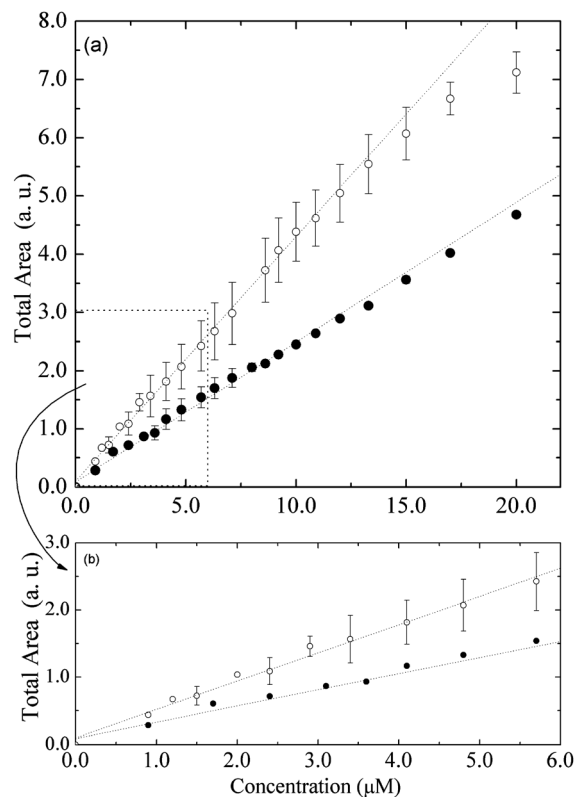


**Fig. 3** (a) Concentration dependence of the total area underneath the emission spectrum of Prodan in water (○) and in cyclohexane (●). As indicated, (b) is an amplification at lower Prodan concentrations.

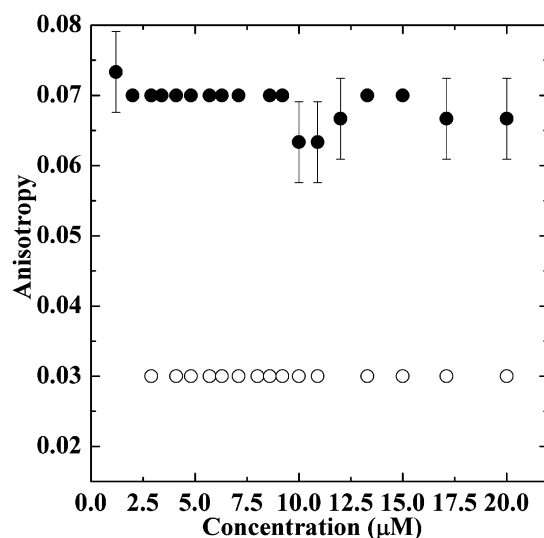


**Fig. 4** Concentration dependence of Prodan steady state fluorescence anisotropy in water (○) and in cyclohexane (●). In water,  $\lambda_{\text{exc}} = 360$  nm and  $\lambda_{\text{em}} = 521$  nm, and in cyclohexane  $\lambda_{\text{exc}} = 340$  nm and  $\lambda_{\text{em}} = 390$  nm. Temperature 25 °C.

monomers. However, opposite to the emission spectra behavior (Fig. 3a, inset), a clear change in the shape of the optical absorption spectrum of Prodan in water is observed at concentrations higher than 6  $\mu\text{M}$ , as shown in Fig. 5a (very similar spectra were obtained for four different samples). At lower

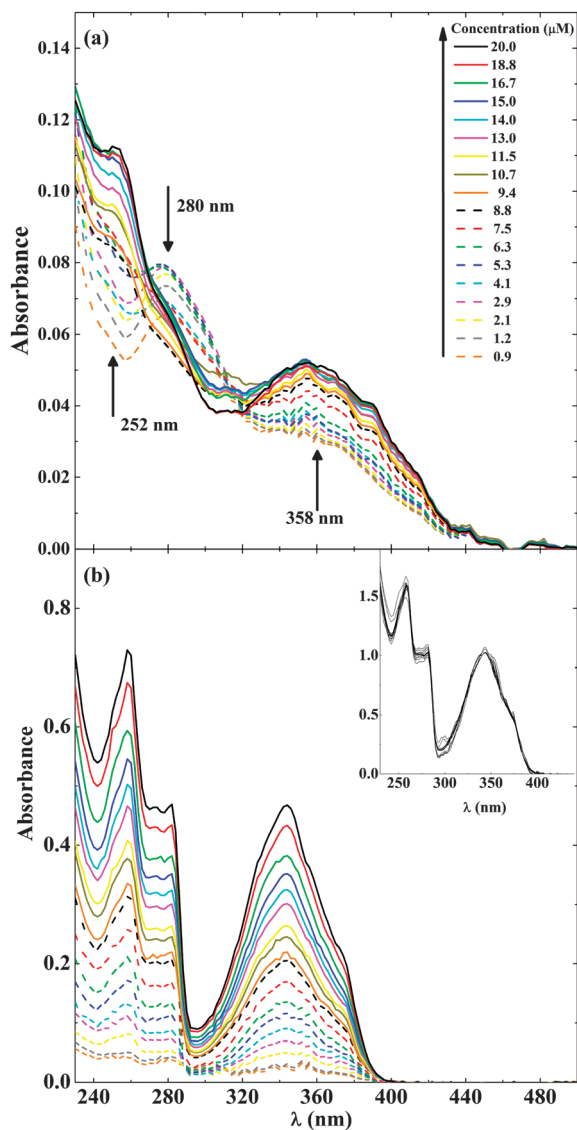


**Fig. 5** Absorption spectrum of Prodan, in water (a) and in cyclohexane (b), for different concentrations. Temperature 25 °C. Optical pathway of 1 cm. Insets show the superposition of normalized spectra at 360 nm in cyclohexane.

concentrations, until  $\sim 6 \mu\text{M}$ , it is possible to observe a band at around 280 nm ( $\lambda_{\text{max}} = 280 \text{ nm}$ ), which tends to disappear at higher concentrations, and another one comes up at around 250 nm ( $\lambda_{\text{max}} = 252 \text{ nm}$ ), and increases up to  $20 \mu\text{M}$ . A lower energy band, around 358 nm, increases as Prodan concentration increases, but seems to saturate at around  $9 \mu\text{M}$ . Changes in the shape of the absorption spectrum indicate that interactions between Prodan molecules are changing when the concentration is increased, leading to alterations in the electronic levels related to light absorption. Moreover, even at the lowest Prodan concentration tested,  $0.9 \mu\text{M}$ , a clear light scattering profile can be observed below the absorption spectrum (light scattering depends on  $\lambda^{-x}$ , where  $x$  depends on the scattering particle dimensions<sup>87</sup>). Due to the presence of the absorption bands, it is impossible to precisely subtract light scattering from the probe absorption spectrum (see ESI†). However, light scattering is

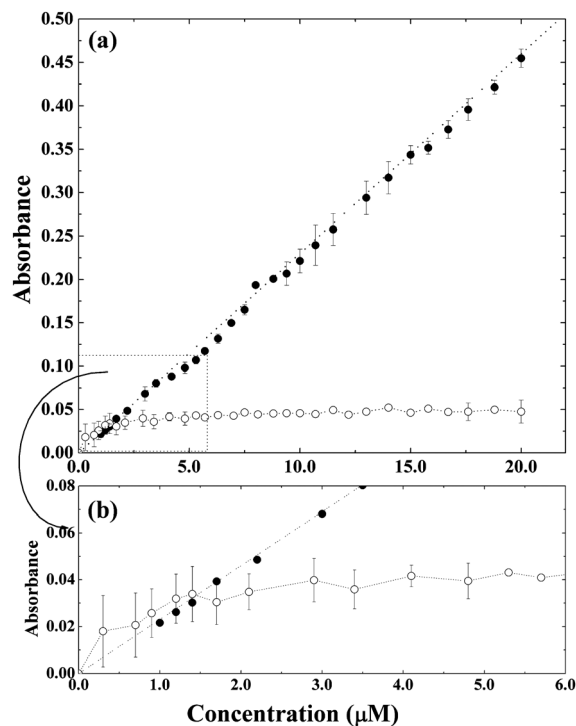


**Fig. 6** (a) Concentration dependence of the absorbance of Prodan in water ( $\circ$ ,  $\lambda = 360 \text{ nm}$ ) and in cyclohexane ( $\bullet$ ,  $\lambda = 340 \text{ nm}$ ). As indicated, (b) is an amplification at lower Prodan concentrations.

strong evidence that there are Prodan aggregates in water at concentrations as low as  $0.9 \mu\text{M}$ , as small monomeric Prodan should not scatter UV or visible light.

For a quantitative analysis of the Prodan optical spectrum, absorbance values at the maximum of the lower energy band (358 nm in water and 344 nm in cyclohexane) were plotted *versus* Prodan concentration (Fig. 6). The lower energy band was chosen as it is less altered by the scattered light (turbidity proportional to  $\lambda^{-x}$ ), which distorts the Prodan spectrum in water. Prodan in cyclohexane shows a linear dependence on the concentration, in accord with the Lambert–Beer law,<sup>87</sup> undoubtedly indicating the presence of the same optical absorption center, from  $0.9$  to  $20 \mu\text{M}$ . Considering this result, together with the absence of light scattered by Prodan in cyclohexane (Fig. 5b), we conclude that there is no aggregation of Prodan in cyclohexane, up to  $20 \mu\text{M}$ .

For Prodan in water, it was not possible to identify a range of concentrations where a linear dependence of absorbance at 358 nm *versus* Prodan concentration could be observed, even at very low Prodan concentrations (see Fig. 6b). As mentioned above, there is an obvious saturation of the absorbance measured at  $\lambda = 358 \text{ nm}$ . Hence, the amount of absorption centers that absorb light at this wavelength at very low concentration ( $0.9 \mu\text{M}$ ) does not increase linearly with Prodan concentration, and could be related to monomeric or aggregated Prodan. As discussed above, there are Prodan aggregates in water at all concentrations studied here, but the dimensions of the aggregates should not change much with Prodan concentration, as samples at all studied concentrations yielded similar fluorescence anisotropy values (Fig. 4, and discussion therein).

To try to understand the optical absorption spectrum of Prodan in water (Fig. 5a), absorption transition energies were calculated for monomers and aggregated Prodan embedded in aqueous solution. The absorption electronic energies for aggregates, with 2–10 Prodan molecules, were calculated and no band shift was observed as the number of molecules increased from 2 to 10, but only an increase in band intensities. For computational reasons, statistical calculations were done with 75 different configurations of two Prodan molecules, obtained from the Prodan liquid simulation. Hence, for both systems, monomers and dimers, 75 QM calculations were performed, and average values for electronic absorption transition energies and the corresponding oscillator strength values (OS) were obtained. These results are presented in ESI.† In Fig. 7, average values for electronic absorption transitions of Prodan monomers and dimers are compared with the experimental absorption spectra obtained at low and high concentrations, 1.2  $\mu\text{M}$  (black line) and 20 (red line)  $\mu\text{M}$ , respectively. Vertical (dashed) lines are calculated energy values, and their heights are proportional to the transition oscillator strength, indicating electronic transition intensities. There is a correlation between the electronic absorption energies calculated for the Prodan monomer and experimental spectra obtained at low concentrations (Fig. 7). Clearly, the low energy absorption band, at around  $29 \times 10^3 \text{ cm}^{-1}$  (approximately corresponding to the 358 nm band), is present in the monomer spectrum only, hence it seems to be due to monomeric Prodan. Accordingly, Fig. 5 and 6 indicate that monomeric Prodan concentration slowly increases as Prodan concentration increases, but absorbance at 358 nm flattens, showing the predominance of aggregated Prodan as concentration increases.

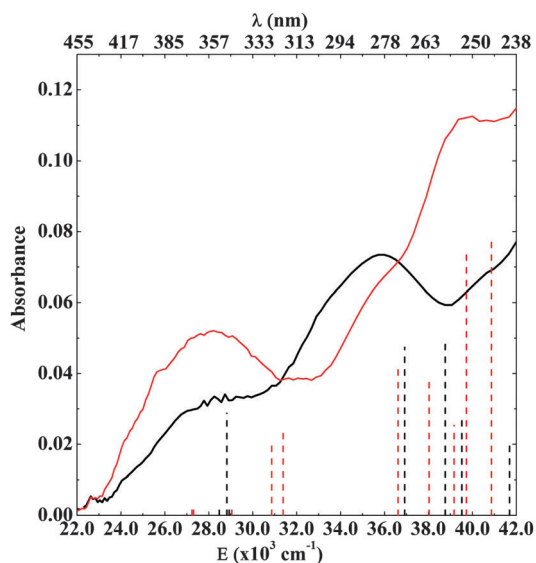


**Fig. 7** Comparison between energy values calculated for electronic transitions of a Prodan monomer (dashed black lines) and aggregates (dashed red lines). The experimental spectra measured at two different concentrations, 1.2  $\mu\text{M}$  (solid black line) and 20.0  $\mu\text{M}$  (solid red line) are presented for comparison. Heights of the vertical lines are proportional to the corresponding transition oscillator strength values. Electronic transitions not shown were found to have negligible oscillator strength values.

Alternatively, in the electronic transitions calculated for Prodan aggregates, two transitions appear at around  $40\text{--}41 \times 10^3 \text{ cm}^{-1}$ , which are present in the aggregated Prodan spectrum only, and they describe the increase in the experimental band at around 250 nm, showing that this band is characteristic of the aggregates. All the other bands are present in both forms, monomer and aggregated Prodan. Considering the experimental spectrum at 1.2  $\mu\text{M}$ , it is possible to see a small shoulder at around  $40 \times 10^3 \text{ cm}^{-1}$  that reaffirms the presence of aggregates at very low concentration, as observed by the presence of the light scattering already discussed in Fig. 5.

### 3.3 Prodan–Prodan and Prodan–water interactions

To further analyze the presence and stability of Prodan aggregates in water, we calculated the solvation free energy of Prodan in water and in liquid Prodan. As used before, the solvation free energy was obtained as the negative value of the annihilation free energy in solution.<sup>83–85</sup> As described in the previous section, the annihilation process was performed in three stages: first, the atomic charges of the Prodan force field were slowly reduced to zero and the electrostatic term of the solvation free energy of Prodan in solution was calculated; then, the attractive term of the Lennard-Jones potential was also removed and the van der Waals term was calculated; and finally, the repulsive term of the Lennard-Jones potential was taken away and the cavitation term was calculated. The results of the calculated solvation free energy of Prodan in water and in liquid Prodan are presented in Table 1 together with the three contribution terms.

Table 1 shows that Prodan solvates better in liquid Prodan ( $\Delta G_{\text{solvation}} = -38.8 \text{ kcal mol}^{-1}$ ) than in water ( $\Delta G_{\text{solvation}} = -29.6 \text{ kcal mol}^{-1}$ ). The electrostatic term of the solvation free energy favors Prodan–water interaction by approximately  $13 \text{ kcal mol}^{-1}$ . However, the van der Waals term favors the Prodan–Prodan interaction by almost the same amount. Therefore, the difference between the two environments comes from the cavitation term, which is the amount of free energy necessary to open a cavity to insert the Prodan molecule in each solvent. In water, this free energy term is much larger than in Prodan liquid. In water, more molecules are displaced to insert the Prodan molecule, hence several water–water hydrogen bonds are broken. This result shows that the Prodan molecule prefers to interact with other Prodan molecules than with water. Hence, this is a strong indication of the presence of Prodan aggregates in water, even at low concentrations of the fluorophore.

**Table 1** Contribution of the electrostatic, van der Waals and cavitation terms for the calculated solvation free energies for Prodan molecules in water and in liquid Prodan. All values are in  $\text{kcal mol}^{-1}$

	In aqueous solution	In liquid Prodan
Electrostatic	$-19.5 \pm 0.6$	$-6.2 \pm 0.2$
van der Waals	$20.3 \pm 0.6$	$33.6 \pm 1.0$
Cavitation	$10.1 \pm 0.3$	$1.0 \pm 0.1$
$\Delta G_{\text{solvation}}$	$-29.6 \pm 1.5$	$-38.8 \pm 1.3$

## 4. Conclusions

The light scattering profile underneath the optical absorption spectrum of Prodan in water clearly indicates the presence of aggregates at very low Prodan concentration (0.9  $\mu\text{M}$  in Fig. 5). Experimental evidence of Prodan aggregation is theoretically supported by electronic transition energy calculations: the optical absorption band at 358 nm is related to the monomeric form of Prodan and the one at 250 nm is related to aggregates (Fig. 7). The 358 nm band saturation and the relative increase in the 250 nm band indicate that aggregated Prodan prevails at higher concentrations, but they are present at all measured concentrations. Prodan aggregation in water is also corroborated by solvation free energy calculations, which showed that Prodan molecules interact preferentially with other Prodan molecules than with water molecules (Table 1).

Considering the non-linear dependence of the intensity of the 358 nm absorption band on Prodan concentration (Fig. 6), it is rather intriguing that the intensity of the Prodan emission spectrum, obtained by excitation at  $\lambda = 358$  nm, would be linear up to around 15  $\mu\text{M}$  (Fig. 3). That certainly deserves further investigation.

Optical spectroscopy, both absorption and emission, clearly indicates that Prodan is monomeric in cyclohexane, at all concentrations studied.

Prodan aggregation in water medium, even at very low concentrations, must be considered when using this fluorescent probe, having in mind that its fluorescence spectrum was found to be rather insensitive to aggregation.

## Acknowledgements

Work partially supported by CNPq, CAPES, FAPESP, INCT-FCx and nBioNet (Brazil). Additionally, C.C.V.-S. acknowledges a fellowship from FAPESP and MTL and KC research fellowships from CNPq.

## References

- 1 S. A. Benner, in *Water and Life*, CRC Press, 2010, pp. 157–175.
- 2 R. A. Nome, *J. Braz. Chem. Soc.*, 2010, **21**, 2189–2204.
- 3 N. T. Hunt, *Chem. Soc. Rev.*, 2009, **38**, 1837–1848.
- 4 M. Brüessel, S. Zahn, E. Hey-Hawkins and B. Kirchner, *Adv. Inorg. Chem.*, 2010, **62**, 111–142.
- 5 S. Patel, in *Modeling Solvent Environments: Applications to Simulations of Biomolecules*, Wiley-VCH Verlag GmbH & Co. KGaA, 2010, pp. 273–308.
- 6 C. Reichardt, *Chem. Rev.*, 1994, **94**, 2319–2358.
- 7 C. Reichardt, *Solvents and Solvent Effects in Organic Chemistry*, 3rd edn, Wiley-VCH, Weinheim, 2004.
- 8 G. Weber and F. J. Farris, *Biochemistry*, 1979, **18**, 3075–3078.
- 9 D. Krilov, M. Balarin, M. Kosovic and J. Brnjac-Kraljevic, *Eur. Biophys. J.*, 2008, **37**, 1105–1110.
- 10 V. Y. Artukhov, O. M. Zharkova and J. P. Morozova, *Spectrochim. Acta, Part A*, 2007, **68**, 36–42.
- 11 C. E. Bunker, T. L. Bowen and Y. P. Sun, *Photochem. Photobiol.*, 1993, **58**, 499–505.
- 12 R. Alleva, G. Ferretti, B. Borghi, E. Pignotti, A. Bassi and G. Curatola, *Transfus. Sci.*, 1995, **16**, 291–297.
- 13 A. Ambrosini, E. Bertoli, F. Tanfani, M. Wozniak and G. Zolese, *Chem. Phys. Lipids*, 1994, **72**, 127–134.
- 14 A. Ambrosini, G. Zolese, G. Balercia, E. Bertoli, G. Arnaldi and F. Mantero, *Fertil. Steril.*, 2001, **76**, 501–505.
- 15 L. A. Bagatolli, B. Maggio, F. Aguilar, C. P. Sotomayor and G. D. Fidelio, *Biochim. Biophys. Acta*, 1997, **1325**, 80–90.
- 16 J. D. Bell, M. Burnside, J. A. Owen, M. L. Royall and M. L. Baker, *Biochemistry*, 1996, **35**, 4945–4955.
- 17 G. Ferretti, M. Taus, N. Dousset, M. L. Solera, P. Valdiguie and G. Curatola, *Biochem. Mol. Biol. Int.*, 1993, **30**, 713–719.
- 18 F. Moyano, J. J. Silber and N. M. Correa, *J. Colloid Interface Sci.*, 2008, **317**, 332–345.
- 19 H. Rottenberg, *Biochemistry*, 1992, **31**, 9473–9481.
- 20 J. W. Zeng and P. L. G. Chong, *Biophys. J.*, 1995, **68**, 567–573.
- 21 C. C. De Vequi-Suplicy, C. R. Benatti and M. T. Lamy, *J. Fluoresc.*, 2006, **16**, 431–439.
- 22 K. A. Kozyra, M. Jozefowicz, J. R. Heldt and J. Heldt, *Z. Naturforsch., A: Phys. Sci.*, 2008, **63**, 819–829.
- 23 G. Gorbenko and V. Trusova, *Biophys. Chem.*, 2011, **154**, 73–81.
- 24 C. Alvarez, I. F. Pazos, M. E. Lanio, D. Martinez, S. Schreier, F. Casallanovo, A. M. Campos and E. Lissi, *Toxicol.*, 2001, **39**, 539–553.
- 25 L. Tavel, C. Moreau, S. Bouhallab, E. C. Y. Li-Chan and E. Guichard, *Food Chem.*, 2010, **119**, 1550–1556.
- 26 X. Y. Mao, P. S. Tong, S. Gualco and S. Vink, *J. Dairy Sci.*, 2012, **95**, 3481–3488.
- 27 M. M. Adams and E. V. Anslyn, *J. Am. Chem. Soc.*, 2009, **131**, 17068–17069.
- 28 D. J. Cowley, *Nature*, 1986, **319**, 14.
- 29 A. R. Lee and K. K. Karukstis, *Abstr. Papers Am. Chem. Soc.*, 2009, **237**, 994–994.
- 30 O. F. Silva, M. A. Fernandez, S. L. Pennie, R. R. Gil and R. H. de Rossi, *Langmuir*, 2008, **24**, 3718–3726.
- 31 R. H. de Rossi, O. F. Silva, R. V. Vico and C. J. Gonzalez, *Pure Appl. Chem.*, 2009, **81**, 755–765.
- 32 K. A. Al-Hassan and M. F. Khanfer, *J. Fluoresc.*, 1998, **8**, 139–152.
- 33 A. B. J. Parusel, F. W. Schneider and G. Kohler, *THEOCHEM*, 1997, **398**, 341–346.
- 34 J. R. Lakowicz and A. Balter, *Biophys. Chem.*, 1982, **16**, 223–240.
- 35 A. M. Rollinson and H. G. Drickamer, *J. Chem. Phys.*, 1980, **73**, 5981–5996.
- 36 J. R. Lakowicz and A. Balter, *Biophys. Chem.*, 1982, **16**, 117–132.
- 37 W. Nowak, P. Adamczak, A. Balter and A. Sygula, *THEOCHEM*, 1986, **139**, 13–23.
- 38 F. Heisel, J. A. Mieke and A. W. Szemik, *Chem. Phys. Lett.*, 1987, **138**, 321–326.
- 39 A. Balter, W. Nowak, W. Pawelkiewicz and A. Kowalczyk, *Chem. Phys. Lett.*, 1988, **143**, 565–570.
- 40 P. Ilich and F. G. Prendergast, *J. Phys. Chem.*, 1989, **93**, 4441–4447.

- 41 J. Catalan, P. Perez, J. Laynez and F. G. Blanco, *J. Fluoresc.*, 1991, **1**, 215–223.
- 42 S. Y. Sun, M. P. Heitz, S. A. Perez, L. A. Colon, S. Bruckenstein and F. V. Bright, *Appl. Spectrosc.*, 1997, **51**, 1316–1322.
- 43 M. Viard, J. Gallay, M. Vincent, O. Meyer, B. Robert and M. Paternostre, *Biophys. J.*, 1997, **73**, 2221–2234.
- 44 A. B. J. Parusel, W. Nowak, S. Grimme and G. Kohler, *J. Phys. Chem. A*, 1998, **102**, 7149–7156.
- 45 A. Parusel, *J. Chem. Soc., Faraday Trans.*, 1998, **94**, 2923–2927.
- 46 A. Kawski, *Z. Naturforsch., A: Phys. Sci.*, 1999, **54**, 379–381.
- 47 R. Adhikary, C. A. Barnes and J. W. Petrich, *J. Phys. Chem. B*, 2009, **113**, 11999–12004.
- 48 A. Kawski, B. Kuklinski and P. Bojarski, *Z. Naturforsch., A: Phys. Sci.*, 2000, **55**, 550–554.
- 49 A. Kawski, B. Kuklinski, P. Bojarski and H. Diehl, *Z. Naturforsch., A: Phys. Sci.*, 2000, **55**, 817–822.
- 50 A. Samanta and R. W. Fessenden, *J. Phys. Chem. A*, 2000, **104**, 8972–8975.
- 51 A. B. J. Parusel, R. Schamschule and G. Kohler, *THEOCHEM*, 2001, **544**, 253–261.
- 52 B. C. Lobo and C. J. Abelt, *J. Phys. Chem. A*, 2003, **107**, 10938–10943.
- 53 K. A. Kozyra, J. R. Heldt, J. Heldt, M. Engelke and H. A. Diehl, *Z. Naturforsch., A: Phys. Sci.*, 2003, **58**, 581–588.
- 54 Y. Huang, X. Y. Li, K. X. Fu and Q. Zhu, *J. Chem. Theory Comput.*, 2006, **5**, 355–374.
- 55 F. Moyano, M. A. Biasutti, J. J. Silber and N. M. Correa, *J. Phys. Chem. B*, 2006, **110**, 11838–11846.
- 56 B. Mennucci, M. Caricato, F. Ingrosso, C. Cappelli, R. Cammi, J. Tomasi, G. Scalmani and M. J. Frisch, *J. Phys. Chem. B*, 2008, **112**, 414–423.
- 57 B. A. Rowe, C. A. Roach, J. Lin, V. Asiago, O. Dmitrenko and S. L. Neal, *J. Phys. Chem. A*, 2008, **112**, 13402–13412.
- 58 S. M. Bakalova and J. Kaneti, *Spectrochim. Acta, Part A*, 2009, **72**, 36–40.
- 59 R. K. Everett, A. A. Nguyen and C. J. Abelt, *J. Phys. Chem. A*, 2010, **114**, 4946–4950.
- 60 W. K. Nitschke, C. C. Vequi-Suplicy, K. Coutinho and H. Stassen, *J. Phys. Chem. B*, 2012, **116**, 2713–2721.
- 61 K. Coutinho and S. Canuto, *Adv. Quantum Chem.*, 1997, **28**, 89–105.
- 62 K. Coutinho, S. Canuto and M. C. Zerner, *J. Chem. Phys.*, 2000, **112**, 9874–9880.
- 63 M. J. Frisch, G. W. Trucks, H. B. Schlegel, G. E. Scuseria, M. A. Robb, J. R. Cheeseman, J. A. Montgomery Jr., T. Vreven, K. N. Kudin, J. C. Burant, J. M. Millam, S. S. Iyengar, J. Tomasi, V. Barone, B. Mennucci, M. Cossi, G. Scalmani, N. Rega, G. A. Petersson, H. Nakatsuji, M. Hada, M. Ehara, K. Toyota, R. Fukuda, J. Hasegawa, M. Ishida, T. Nakajima, Y. Honda, O. Kitao, H. Nakai, M. Klene, X. Li, J. E. Knox, H. P. Hratchian, J. B. Cross, V. Bakken, C. Adamo, J. Jaramillo, R. Gomperts, R. E. Stratmann, O. Yazyev, A. J. Austin, R. Cammi, C. Pomelli, J. W. Ochterski, P. Y. Ayala, K. Morokuma, G. A. Voth, P. Salvador, J. J. Dannenberg, V. G. Zakrzewski, S. Dapprich, A. D. Daniels, M. C. Strain, O. Farkas, D. K. Malick, A. D. Rabuck, K. Raghavachari, J. B. Foresman, J. V. Ortiz, Q. Cui, A. G. Baboul, S. Clifford, J. Cioslowski, B. B. Stefanov, G. Liu, A. Liashenko, P. Piskorz, I. Komaromi, R. L. Martin, D. J. Fox, T. Keith, M. A. Al-Laham, C. Y. Peng, A. Nanayakkara, M. Challacombe, P. M. W. Gill, B. Johnson, W. Chen, M. W. Wong, C. Gonzalez and J. A. Pople, *GAUSSIAN*, Gaussian, Inc., Wallingford, CT, 2004.
- 64 J. Ridley and M. Zerner, *Theor. Chim. Acta*, 1973, **32**, 111–134.
- 65 M. C. Zerner, *INDO/UF: A semi-empirical package*, University of Florida, Gainesville, FL 32611, USA, 2000.
- 66 K. Coutinho and S. Canuto, *DICE: A Monte Carlo program for molecular liquid simulation*, São Paulo, Brazil, 2003.
- 67 N. Metropolis, A. W. Rosenbluth, M. N. Rosenbluth, A. H. Teller and E. Teller, *J. Chem. Phys.*, 1953, **21**, 1087–1092.
- 68 N. Metropolis and S. Ulam, *J. Am. Stat. Assoc.*, 1949, **44**, 335–341.
- 69 M. S. Allen and D. J. Tildesley, *Computer Simulations of Liquids*, Oxford Science Publications, Oxford, 1991.
- 70 A. D. Becke, *Phys. Rev. A*, 1988, **38**, 3098–3100.
- 71 C. T. Lee, W. T. Yang and R. G. Parr, *Phys. Rev. B: Condens. Matter Mater. Phys.*, 1988, **37**, 785–789.
- 72 R. Ditchfield, W. J. Hehre and J. A. Pople, *J. Chem. Phys.*, 1971, **54**, 724–728.
- 73 W. L. Jorgensen, D. S. Maxwell and J. TiradoRives, *J. Am. Chem. Soc.*, 1996, **118**, 11225–11236.
- 74 C. Moller and M. S. Plesset, *Phys. Rev.*, 1934, **46**, 0618–0622.
- 75 M. L. Leininger, W. D. Allen, H. F. Schaefer and C. D. Sherrill, *J. Chem. Phys.*, 2000, **112**, 9213–9222.
- 76 T. H. Dunning, *J. Chem. Phys.*, 1989, **90**, 1007–1023.
- 77 H. J. C. Berendsen, J. P. M. Postma, W. F. van Gunsteren and J. Hermans, in *Intermolecular Forces*, ed. B. Pullman, Reidel, Dordrecht, 1981, pp. 331–342.
- 78 R. W. Zwanzig, *J. Chem. Phys.*, 1954, **22**, 1420–1426.
- 79 A. E. Mark, in *Encyclopedia of Computational Chemistry*, ed. P. R. Schleyer, John Wiley & Sons, New York, 1998, vol. 2, pp. 1070–1083.
- 80 D. A. Pearlman and B. G. Rao, in *Encyclopedia of Computational Chemistry*, ed. P. R. Schleyer, John Wiley & Sons, New York, 1998, vol. 2, pp. 1036–1061.
- 81 W. L. Jorgensen and C. Ravimohan, *J. Chem. Phys.*, 1985, **83**, 3050–3054.
- 82 W. L. Jorgensen, in *Encyclopedia of Computational Chemistry*, ed. P. R. Schleyer, John Wiley & Sons, New York, 1998, vol. 2, pp. 1061–1070.
- 83 H. C. Georg, K. Coutinho and S. Canuto, *Chem. Phys. Lett.*, 2005, **413**, 16–21.
- 84 H. Pasalic, A. J. A. Aquino, D. Tunega, G. Haberhauer, M. H. Gerzabek, H. C. Georg, T. F. Moraes, K. Coutinho, S. Canuto and H. Lischka, *J. Comput. Chem.*, 2010, **31**, 2046–2055.
- 85 W. L. Jorgensen, J. K. Buckner, S. Boudon and J. Tiradorives, *J. Chem. Phys.*, 1988, **89**, 3742–3746.
- 86 J. R. Lakowicz, *Principles of Fluorescence Spectroscopy*, 3rd edn, Plenum Publishers, New York, 2006.
- 87 C. R. Cantor and P. R. Schimmel, *Part II: Techniques for the study of biological structure and function*, W.H. Freeman and Company, New York, 1980.